

The immediate environment of the Class 0 protostar VLA1623, on scales of ~ 50 – 100 AU, observed at millimetre and centimetre wavelengths

D. Ward-Thompson^{1*}, J. M. Kirk¹, J. S. Greaves², P. André³

¹*School of Physics and Astronomy, Cardiff University, Cardiff, CF24 3AA*

²*School of Physics and Astronomy, St Andrews University, North Haugh, St Andrews, Fife, KY16 9SS*

³*Laboratoire AIM, DSM/IRFU/Service d'Astrophysique, CEA Saclay, 91191 Gif-sur-Yvette, France*

19 January 2013

ABSTRACT

We present high angular resolution observations, taken with the Very Large Array (VLA) and Multiple Element Radio Linked Interferometer Network (MERLIN) radio telescopes, at 7 mm and 4.4 cm respectively, of the prototype Class 0 protostar VLA1623. At 7 mm we detect two sources (VLA1623A & B) coincident with the two previously detected components at the centre of this system. The separation between the two is 1.2 arcsec, or ~ 170 AU at an assumed distance of 139 pc. The upper limit to the size of the source coincident with each component of VLA1623 is ~ 0.7 arcsec, in agreement with previous findings. This corresponds to a diameter of ~ 100 AU at an assumed distance of 139 pc. Both components show the same general trend in their broadband continuum spectra, of a steeper dust continuum spectrum shortward of 7 mm and a flatter spectrum longward of this.

We estimate an upper limit to the VLA1623A disc mass of $\leq 0.13 M_{\odot}$ and an upper limit to its radius of ~ 50 AU. The longer wavelength data have a spectral index of $\alpha \sim 0.6 \pm 0.3$. This is too steep to be explained by optically thin free-free emission. It is most likely due to optically thick free-free emission. Alternatively, we speculate that it might be due to the formation of larger grains or planetesimals in the circumstellar disc. We estimate the mass of VLA1623B to be $\leq 0.15 M_{\odot}$. We can place a lower limit to its size of $\sim 30 \times 7$ AU, and an upper limit to its diameter of ~ 100 AU. The longer wavelength data of VLA1623B also have a spectral index of $\alpha \sim 0.6 \pm 0.3$. The nature of VLA1623B remains a matter of debate. It could be a binary companion to the protostar, or a knot in the radio jet from VLA1623A.

Key words: stars: formation – protostars – interferometry

1 INTRODUCTION

Young stellar objects (YSOs) are divided observationally into a number of different classes. Class 0 protostars represent the earliest observed phase of protostellar evolution (André, Ward-Thompson & Barsony, 1993; hereafter AWB93), in which the protostar has accumulated less than half of its final main-sequence mass. The subsequent Class I phase (Lada 1987; Wilking, Lada & Young 1989) occurs when the protostar accumulates the majority of the remainder of its mass. By the time of the Class II phase (Lada 1987; Wilking et al., 1989), the large-scale envelope seems to have entirely accreted onto the protostar or its circumstellar disc (e.g. Ward-Thompson, André & Lay 2004; Ward-Thompson

2007). This phase generally correlates with the ‘classical’ T Tauri stage (André & Montmerle 1994).

There remain some aspects of protostellar evolution that are still a matter of debate. For example, the epoch of circumstellar disc formation is not precisely known, and the time of the onset of planet formation within the disc is also highly uncertain. There are as yet insufficient observations to tie down the beginnings of these important phases. Furthermore, the effect of binarity on this simple picture is not fully understood.

Indirect evidence for the presence of a disc is usually implied from the presence of a bipolar jet or outflow (e.g. Curiel et al. 2006; Torrelles et al. 2011), and jets and outflows have been observed in the Class 0 stage (e.g. Bontemps, Ward-Thompson & André 1996; André, Ward-Thompson & Barsony, 2000 – hereafter AWB00). In fact, bipolar outflows

* e-mail: D.Ward-Thompson@astro.cf.ac.uk

become less energetic and less well collimated with age (Henriksen, André & Bontemps 1997). Consequently, it is implied that discs must form in the earliest protostellar stages. There is also evidence that they are threaded by magnetic fields (Holland et al. 1996; Girart et al. 2006).

Single-dish observations with current mm telescopes typically provide resolutions of order 1000–2000 AU in nearby star-forming regions, and so probe circumstellar envelopes. Interferometers can reach scales below 100 AU, and so can probe the structure of circumstellar discs (e.g. Guiloteau et al. 2008; Dutrey et al. 2008; Schaefer et al. 2009). A comparison between interferometer data and single-dish data allow one to assess the relative importance of circumstellar discs and envelopes (Ward-Thompson 2007). For Class 0 protostars the disc contains typically ≤ 20 –25% of the total mm flux. For Class I sources this value is typically around $\sim 25\%$. For Class II sources, typically all of the mm flux arises from the disc (Ward-Thompson et al., 2004; Ward-Thompson 2007).

VLA 16234-2417 (hereafter VLA1623) was the first Class 0 object to be recognised, and it is still one of the youngest known members of this class (AWB93). VLA1623 has a jet (Bontemps & André 1997), a bipolar CO outflow (André et al., 1990; Dent et al., 1995), and evidence for a circumstellar disc (Pudritz et al., 1996). This would indicate that discs, like jets and outflows, are formed at the very beginning of protostellar evolution.

Subsequent observations at 2.7 mm suggested that VLA1623 was in fact a binary protostar, and that a source which had previously been identified as a knot in the jet was in fact a second protostellar component (Looney, Mundy & Welch, 2000; 2003). Somewhat confusingly, the second component was originally known as ‘knot A’ of the jet (Bontemps & André 1997), and was then renamed ‘component B’ of the protostar (Looney et al., 2000). We follow the more recent naming system and refer to the originally known protostar as VLA1623A, and to the second component to the west as VLA1623B, after Looney et al., (2000).

A number of circumstellar discs have now been imaged around young stars, although the majority of those studied have been more evolved pre-main sequence stars. For example, Qi et al. (2004) imaged the disc around the Class II source TWHya, and found it to be consistent with a disc in Keplerian rotation.

The question as to when planets begin to form in discs is also very much a matter for debate. A low-mass companion was found in the disc of the Class II protostar HL Tau (Welch et al., 2004). It has recently been hypothesised that this may be a planet in the process of formation (Greaves et al., 2008). If so, then this indicates that planets, or at least planetesimals, have started to form by the Class II stage. However, subsequent work on HL Tau did not see the companion source (Carrasco-Gonzalez et al. 2009).

Planetesimal literally means a piece of a planet. Typical sizes of planetesimals are kilometer-sized or larger. These are the building blocks of the rocky planets like the Earth, and also of the cores of gas giants such as Jupiter. One problem in our understanding of the formation of planetesimals is that of drag between the gas and the solids.

The size of a solid particle will determine how it is affected by drag (Brauer et al., 2008). Dust grains of a millimetre or less in diameter will co-orbit with the gas. How-

ever, objects of centimetre to metre size experience significant drag from the surrounding gas. Models predict that such objects would rapidly lose angular momentum and spiral into the central star. Objects significantly larger than this, namely planetesimals of kilometre size or greater, have sufficient inertia that they are effectively immune to drag. Collisional fragmentation is also a potential barrier to grain growth (Brauer et al., 2008). Therefore, whatever process takes material from millimetre to kilometre sizes must occur fairly rapidly otherwise all of the material would end up in the central star.

There are very few observations of large grains or planetesimals in discs to constrain these models. The peak of their emission should be shifted to longer wavelengths relative to ‘normal’ inter-stellar dust grains. Hence, it is necessary to search for them at mm and cm wavelengths. In this paper we present high angular resolution observations of VLA1623, that were taken in the mm and cm regimes, in order to probe the immediate environment of the protostar itself and study its disc, at this very earliest stage of protostellar evolution.

2 OBSERVATIONS

We present data from the Very Large Array (VLA) radio telescope, which consists of 27 radio antennas in a Y-shaped configuration, located near Socorro, New Mexico, in the USA. Each antenna is 25 m in diameter. The antennas can be moved from a dispersed configuration (A array) with a maximum baseline of 36 km, to a compact configuration with a maximum baseline of 1 km (D array). We show previously unpublished data from the VLA archive. The data were taken on 2004 February 1 in B/C configuration (~ 4 –10-km baselines), and on 2005 July 29 in C array (3.6 km maximum baseline), at a wavelength of 7mm (43GHz).

The data were reduced in the standard fashion, using the software package AIPS (Bridle & Greisen, 1994). Natural beam weighting was used and 500 cleaning iterations were carried out. Phase reference calibration was performed using the standard reference source 16258-25276. The flux calibrator used was 1331+305. The final full-width at half maximum (FWHM) beam-size of the data was 1.0×0.4 arcsec, at a position angle of 33 degrees. The 1-sigma rms noise on the final map was found to be 0.2 mJy/beam.

We also obtained data from the Multiple Element Radio Linked Interferometer Network (MERLIN) at a wavelength of 4.4cm (6.8GHz). MERLIN is an array of six observing stations that together form a telescope with an effective aperture diameter of over 217 kilometres, whose control centre is based at Jodrell Bank, near Manchester, in the UK. Observations were taken on several days between 2009 January 23 and February 24. A total of 37 hours of on-source integration time was taken.

The very low declination of the source (-24 degrees) meant that the source was only visible to MERLIN for a few hours each day, and never rose higher than an elevation of 14 degrees. Subsequently, it was found that the data at each end of every track was of much lower signal to noise ratio than the rest. In addition, some parts of some tracks also suffered from significantly lower than average signal to noise ratio, due to the low elevation of the source. These data were

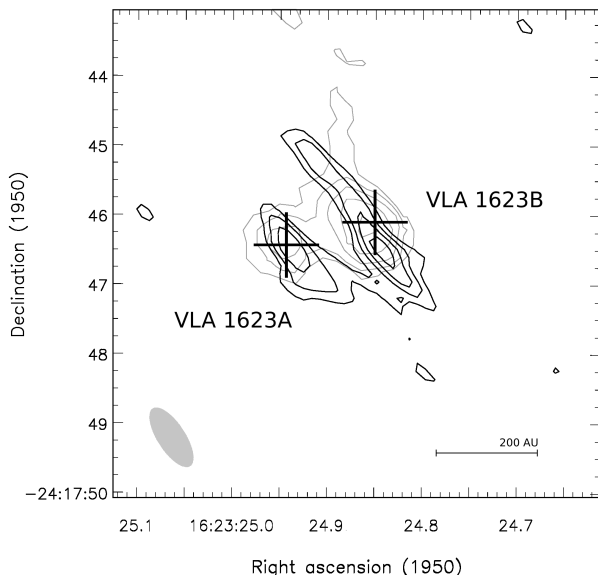


Figure 1. Isophotal contour map of the new 7-mm data of VLA1623, plotted in 1950.0 coordinates for ease of comparison with older data. The lowest contour is at 3σ , and the contour interval is 1σ . The 1σ level of the map is 0.2 mJy/beam. The lighter grey overlaid contours are the 3.6-cm data of Bontemps & André (1997). The position of the VLA1623A protostar is marked with a cross, as is the source immediately to the west, labelled VLA1623B (originally known as ‘knot A’). The peak positions of the two sources at 7 mm are R.A.(1950) = $16^{\text{h}}23^{\text{m}}24.935^{\text{s}}$, Dec.(1950) = $-24^{\circ}17'46.5''$ for VLA1623A, and R.A.(1950) = $16^{\text{h}}23^{\text{m}}24.840^{\text{s}}$, Dec.(1950) = $-24^{\circ}17'46.5''$ for VLA1623B. The beam-size for the 7-mm data is 1.0×0.4 arcsec, at a position angle of 33 degrees, and is shown as a grey ellipse in the lower left-hand corner (the beam-size for the 3.6-cm data was 1.0×0.75 arcsec, at a position angle of 26 degrees). A scale bar of 200 AU is shown at lower right.

discarded, leaving data of total integration time ~ 25 hours. The standard source 1622-253 was used for phase and amplitude calibration. Natural beam weighting was used. The final FWHM beam-width of the data was found to be $\sim 0.2 \times 0.05$ arcsec, at position angle 9 degrees. The 1-sigma rms noise level in the final map was seen to be ~ 80 μ Jy/beam.

The infra-red source S1 was also in our mapped area (Wilking et al., 1989). This is known to be a young magnetic B3 star, and is a radio source sometimes referred to as LFAM11 (Leous et al., 1991). In radio observations it is seen to have a core-halo structure, with synchrotron emission coming from the star’s magnetosphere, and free-free emission from the surrounding compact HII region. The MERLIN observations are more likely to be sensitive to the core component. This is seen to have a flat spectrum between 2 cm and 6 cm, with a flux density of ~ 8 mJy throughout this range (André et al., 1988). We detected LFAM11 strongly in our data, and recovered a 4.4-cm flux density of ~ 6 mJy, consistent with the earlier data. This gave us added confidence that the data taking and reduction methods had all worked correctly, despite the difficulty of observing at this low declination, and from this we estimate that the absolute calibration accuracy of our MERLIN data is ~ 25 – 30% .

3 RESULTS

Figure 1 shows the 7-mm VLA map of VLA1623 as an isophotal contour map. Two sources are seen in the image, with the western source appearing marginally more extended, while the eastern source is more point-like. The apparent extension of both sources in a north-easterly to south-westerly direction is simply a product of the beam shape of these data. The beam is shown as a grey ellipse in the lower left-hand corner.

The flux density of the western source is 2.0 ± 0.2 mJy, while that of the eastern source is 1.2 ± 0.2 mJy. Superposed on Figure 1, in lighter grey contours, are the 3.6-cm VLA data of Bontemps & André (1997). These data also show two sources, with the western source having a 3.6-cm flux density of 0.40 ± 0.02 mJy, and the eastern source being 0.13 ± 0.02 mJy. All of these flux densities are listed in Table 1.

The crosses on Figure 1 show the positions of the two components of the system, A & B, identified at 2.7 mm by Looney et al., (2000). Once again we see that these components are coincident with the two sources we have detected at 7 mm. Hence we see that we have detected both components, and resolved them from one another in the 7-mm data.

The eastern component is agreed by all to be the centre of the protostar VLA1623, which we shall refer to hereafter as VLA1623A (after Looney et al., 2000). The nature of the second component has been a matter of debate. Bontemps & André (1997) hypothesised that it was a knot of the jet emanating from the protostar. Looney et al., (2000) suggested it was a second protostar, which they called VLA1623B. We follow the latter naming system and hereafter refer to the western source as VLA1623B. We note that the position of VLA1623A remains constant to within the astrometric accuracy of the different interferometers. However, the position of VLA1623B appears to move slightly with wavelength. We return to this point below.

The total broadband continuum spectrum of all of VLA1623 was shown by AWB93 (see also André 1994). They fitted all of the data shortward of 2 mm with a single temperature modified blackbody, sometimes known as a greybody. The monochromatic flux density, S_ν , of a greybody, at frequency ν , radiated into solid angle Ω , is given by

$$S_\nu = \Omega f B_\nu(T) [1 - e^{-(\nu/\nu_c)^\beta}], \quad (1)$$

where $B_\nu(T)$ is the blackbody function, ν_c is the frequency at which the optical depth is unity, Ω is the solid angle of the aperture, f is the filling factor of the source within the aperture and β is the dust emissivity index. The spectral index, α , of a function on such a curve is given by

$$\alpha = \frac{\log(S_1/S_2)}{\log(\nu_1/\nu_2)}, \quad (2)$$

where S_1 and S_2 are the flux densities at frequencies ν_1 and ν_2 respectively. In the long wavelength limit, for a given temperature, T , the blackbody function tends to

$$B_\nu \propto \nu^2, \quad (3)$$

which is known as the Rayleigh-Jeans limit. This is true in the mm wavelength regime. In addition, if the emission is

Table 1. Data for the two components of VLA1623. The flux densities are quoted in mJy and measured in aperture sizes of 0.95×0.4 arcsec, 1.0×0.4 arcsec and 1.0×0.75 arcsec at 2.7 mm, 7 mm and 3.6 cm respectively. The upper limits at 4.4 cm are measured in an interferometer beam size of 0.2×0.05 arcsec, and hence the interferometer may have resolved away much of the flux density. All flux densities are quoted to 2 s.f. and all errors to 1 s.f. The 2.7-mm data are from Looney et al. (2000), and the 3.6-cm data are from Bontemps & André (1997). The spectral index at 2.7 mm α_{mm} is taken to be 3.5, as for the whole of VLA1623 (AWB93). This was subtracted from the longer wavelength flux densities, and a spectral index at cm wavelengths α_{cm} was calculated for the residual flux densities. The masses were simply estimated by scaling the 2.7-mm flux densities to the total VLA1623 flux density (see text for discussion).

| Source | VLA1623A | VLA1623B |
|----------------------|-----------------|-----------------|
| $S_{2.7mm}$ (mJy) | 22 ± 4 | 26 ± 4 |
| S_{7mm} (mJy) | 1.2 ± 0.2 | 2.0 ± 0.2 |
| $S_{3.6cm}$ (mJy) | 0.13 ± 0.02 | 0.40 ± 0.02 |
| $S_{4.4cm}$ (mJy) | ≤ 0.24 | ≤ 0.24 |
| α_{mm} | 3.5 ± 0.3 | 3.5 ± 0.3 |
| α_{cm} | 0.6 ± 0.3 | 0.6 ± 0.3 |
| Mass (M_{\odot}) | ≤ 0.13 | ≤ 0.15 |

also optically thin ($\nu \ll \nu_c$), which it usually is for cold dust in the mm regime, then

$$S_{\nu} \propto \nu^{2+\beta}, \quad (4)$$

from which we see that β is related to the spectral index α in the mm by the equation

$$\alpha = 2 + \beta. \quad (5)$$

Hence a single-temperature, optically-thin greybody will produce a straight line on a plot of $\log(S_{\nu})$ versus $\log(\nu)$ in the mm regime. AWB93 and André (1994) found temperatures of 15–20 K, with $\beta = 1.5 \pm 0.3$ for the whole of VLA1623.

If we assume that the mm integrated flux density is optically thin, then the mass, M , of the gas and dust can be calculated using the following equation

$$M = \frac{S_{\nu} D^2}{\kappa_{\nu} B_{\nu}}, \quad (6)$$

where D is the distance to the source and κ_{ν} is the mass opacity of the gas (c.f. André & Montmerle 1994; Kirk, Ward-Thompson & André 2005). We typically use a value of $\kappa_{1.3mm} = 0.01 \text{ cm}^2 \text{ g}^{-1}$ (see e.g. Simpson et al. 2008 and references therein). Using this method, AWB93 found a mass of $0.6 M_{\odot}$ within a 2000 AU diameter aperture around VLA1623.

3.1 VLA1623A

We can place an upper limit on the size of the emission from the protostar VLA1623A of 0.7 arcsec, or 100 AU, at an assumed distance of 139 pc (Mamajek 2008; Simpson, Nutter & Ward-Thompson 2008), based on the 7-mm data presented in Figure 1. The projected distance between VLA1623A and B is 1.2 arcsec, corresponding to a projected separation of 170 AU.

Pudritz et al. (1996) discovered a compact mm/submm

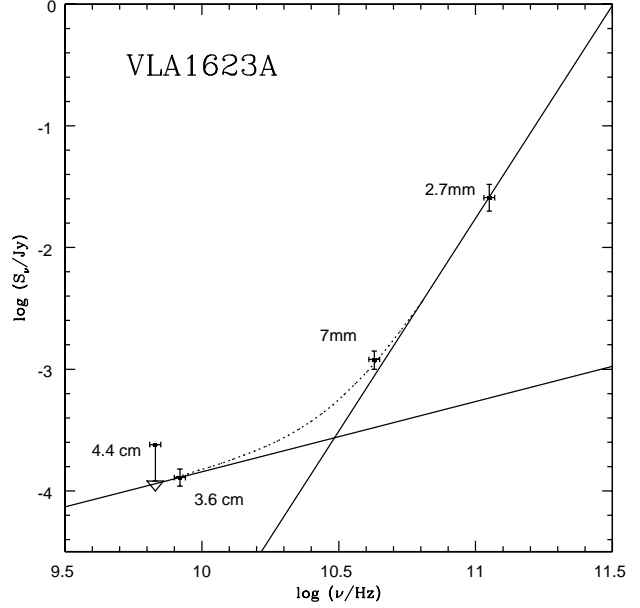


Figure 2. Broadband spectrum of the source VLA1623A only, plotted as log flux density, S_{ν} , versus log frequency, ν . Flux densities were measured in each case on the compact source (see Table 1). This is speculated to be a circumstellar disc of radius ~ 50 AU. Note that a single straight line cannot fit the data. The steeper of the two solid lines has $\alpha=3.5$ and $\beta=1.5$, consistent with the fit found for the whole of VLA1623 (AWB93), normalised to the 2.7-mm flux density. The flatter of the two solid lines has $\alpha=0.6$. The dotted line is the sum of the two. Data are taken from: 7 mm & 4.4 cm – this paper; 3.6 cm – Bontemps & André (1997); 2.7 mm – Looney et al., (2000).

source at the position of the protostar VLA1623A at 0.85 and 1.3 mm, using the James Clerk Maxwell Telescope (JCMT) and Caltech Submillimetre Observatory (CSO) as a two-dish interferometer. This source was unresolved in their observations. They were able to place an upper limit on the diameter of this source of ~ 0.8 arcsec. They derived a different actual size because they assumed a different distance. However, Looney et al. (2000) claimed that the data could not rule out VLA1623 being a binary source, due to the sparse u-v plane coverage of the JCMT-CSO interferometer.

We postulate that the source we see at the position of the VLA1623A protostar, with an upper limit diameter of 0.7 arcsec, is a circumstellar disc around VLA1623A. We do not resolve this source. However, we note that the upper limit radius of this suggested disc is 50 AU, consistent with the sizes of discs around other young stellar objects (e.g. Qi et al., 2004). The outflow from VLA1623A is almost exactly in the plane of the sky (André et al., 1990; Dent et al., 1995), so if this source is a disc, we are probably seeing it close to edge-on.

Figure 2 shows the broad-band spectrum of the compact VLA1623A protostar source on its own, as a plot of log flux density against log frequency. The data-points from Bontemps & André (1997), and Looney et al., (2000) are

plotted on the same graph as the flux density measured for the eastern source in Figure 1 (see also Table 1). We did not detect VLA1623A at 4.4 cm with MERLIN, with a $1\text{-}\sigma$ error-bar on the data of $\sim 80\text{ }\mu\text{Jy/beam}$ at this wavelength. This is shown as a $3\text{-}\sigma$ upper limit on Figure 2.

However, we see that a single straight line does not fit the data. Therefore, even on scales of 50 AU radius around the protostar VLA1623A itself, there is more than one emission mechanism at work. This is to be expected. The disc will contribute thermal dust emission. Similarly, there is predicted to be a shock at the protostellar surface, which should produce free-free emission. Alternatively, there could be optically thick free-free emission from the base of the shock-ionized jet.

We cannot constrain the short wavelength spectral index, so we assume that it has the same value as that for the whole of VLA1623, namely $\alpha=3.5$ and $\beta=1.5$ (AWB93). We acknowledge that this assumption may not be valid, but it is the best assumption that can be made with the available data. A grey-body function with these values is shown as the steeper of the two solid lines on Figure 2, where it has simply been normalised to fit the 2.7-mm data.

The extrapolation of this curve was subtracted from the 7-mm and 3.6-cm data, and the residual flux densities were fitted with a straight-line fit. We refer to these residual flux densities as the dust-corrected flux densities. The fitted straight-line is shown as the shallower of the two solid lines on Figure 2. This line has a spectral index $\alpha\sim 0.6$. The dotted line shows the sum of the two solid lines. The dust spectrum only contributes a very small percentage to the 3.6-cm flux density. Similarly, the shallow line only contributes a negligible percentage to the 2.7-mm flux density. We note that the 7-mm data-point lies close to the break in the spectrum, and hence is crucial to its understanding. The whole of VLA1623 also has a spectral break at around this point (André 1994). The 4.4-cm upper limit lies above the fit to the cm spectrum, so cannot constrain the spectral index.

If the mass of VLA1623A simply scaled with its 2.7-mm flux density relative to the mass of the whole of VLA1623, then the circumstellar disc around VLA1623A would have a mass of $\leq 0.13\text{ }M_{\odot}$. However, note that this assumes that the temperature of the emitting dust remains the same from scales of 2000 AU down to scales of ~ 100 AU. It will probably be warmer, and hence the mass will be lower. However, this also makes the assumption that the dust mass opacity remains the same across these different size-scales. This would not be true if there were significant grain growth in the disc. Pudritz et al. (1996) found a lower limit to the disc mass of VLA1623A of $\sim 0.03\text{ }M_{\odot}$, and Looney et al. (2000) derive a lower limit of $\sim 0.04\text{ }M_{\odot}$, consistent with our results.

The best-fit straight line to the 7-mm and 3.6-cm data has $\alpha=0.6$. This is greater than the spectral index of optically thin free-free emission, which should be closer to -0.1 . It could be that the free-free emission is optically thick, and could arise at the base of the jet (Wright & Barlow 1975; Reynolds 1986). Alternatively, this excess could be due to a population of larger grains, or planetesimals, growing in the disc around the protostar VLA1623A (c.f. Greaves et al. 2008).

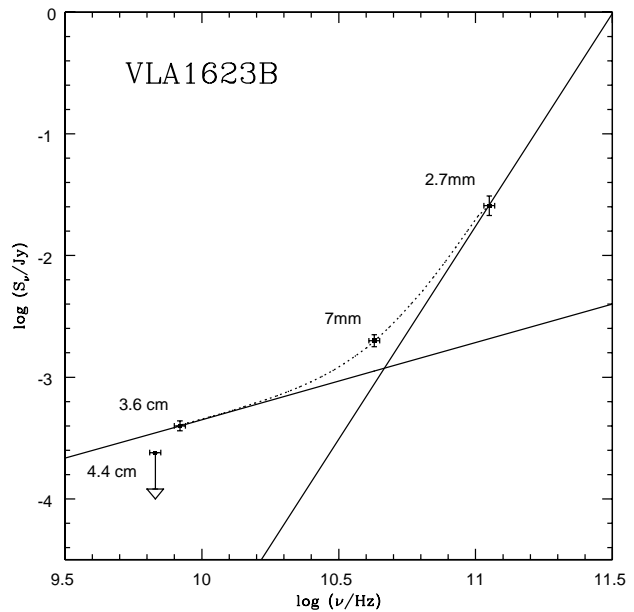


Figure 3. Broadband spectrum of the source VLA1623B only, plotted as log flux density, S_{ν} , versus log frequency, ν . Flux densities were measured in each case on the western source (see Table 1). Note how once again a single straight line cannot fit the data. The steeper of the two solid lines has $\alpha=3.5$ and $\beta=1.5$, consistent with the fit found for the whole of VLA1623 (AWB93), normalised to the 2.7-mm flux density. The flatter of the two solid lines has $\alpha=0.6$. The dotted line is the sum of the two. Data are taken from: 7 mm – this paper; 3.6 cm – Bontemps & André (1997); 2.7 mm – Looney et al., (2000).

3.2 VLA1623B

Figure 3 shows the broad-band continuum spectrum of the compact western source VLA1623B, as a plot of log flux density against log frequency. The data-points from Bontemps & André (1997) and Looney et al. (2000) are plotted on the same graph as the flux density measured for this source in Figure 1 (see also Table 1).

Again we see that a single straight line does not fit the data. So again there must be more than one emission mechanism at work. We cannot constrain the short wavelength spectral index, so we assume that it has the same value as that for the whole of VLA1623, namely $\alpha=3.5$ and $\beta=1.5$ (AWB93), as before. A grey-body function with these values is shown as the steeper of the two solid lines on Figure 3, where it has been normalised to fit the 2.7-mm data.

The extrapolation of this curve was subtracted from the 7-mm and 3.6-cm data, and the residual dust-corrected flux densities were fitted with a straight-line fit, as before. The fitted straight-line is shown as the shallower of the two solid lines on Figure 3. This line has a spectral index $\alpha=0.6$. The dotted line shows the sum of the two solid lines. The dust spectrum only contributes a very small percentage to the 3.6-cm flux density. Similarly, the shallow line only contributes a negligible percentage to the 2.7-mm flux density.

If the mass of VLA1623B simply scaled with its 2.7-mm

flux density relative to the mass of the whole of VLA1623, then VLA1623B would have a mass of $\leq 0.15 M_{\odot}$. Once again we note that this assumes that the temperature of the emitting dust remains the same from scales of 2000 AU down to scales of ~ 100 AU. It also makes the assumption that the dust mass opacity remains the same across these different size-scales.

We did not detect VLA1623B at 4.4 cm with MERLIN, with a $1\text{-}\sigma$ error-bar on the data of $\sim 80 \mu\text{Jy/beam}$ at this wavelength. This is shown as a $3\text{-}\sigma$ upper limit on Figure 3. We see that this lies below the extrapolated fit to the cm flux densities. Hence, VLA1623B cannot be a compact source relative to our beam. This would suggest that the source is extended relative to our beam of $\sim 0.2 \times 0.05$ arcsec, which is approximately $\sim 30 \times 7$ AU. This puts a lower limit to the size of VLA1623B.

4 DISCUSSION

The nature of VLA1623B remains a matter for debate. It is either a binary protostar component, as suggested by Looney et al. (2000), or it is a knot in the radio jet, as suggested by Bontemps & André (1997). We now summarise the evidence for and against each of these hypotheses.

4.1 Binary protostar?

The case for VLA1623 being a binary protostar appears strong when one looks at the 2.7-mm data (Looney et al. 2000). The sources appear to be of similar size and have similar flux densities at this wavelength. Likewise, the similarity of their cm spectral indices appears to indicate that these two sources are the same type of object.

However, the nature of such a binary must be somewhat more complex than our simple ideas would predict. For example, one might normally expect the two components of a binary system to have similar angular momenta. In this case the outflow from VLA1623A is directed roughly towards VLA1623B. Hence the presumed disc around VLA1623A cannot be co-planar with the line joining VLA1623A & B, which would be the plane of their mutual orbits. Therefore, the angular momentum of the VLA1623A disc would be misaligned relative to the angular momentum of the putative binary protostar.

This does not preclude this hypothesis. Other misaligned jets in binary systems have been observed (e.g. Albrecht et al. 2009). They have also been modelled (e.g. Stamatellos et al., 2011; Walsh et al., in prep). However, it does mean that it is not a simple binary protostellar system.

4.2 Knot in the jet?

The case for VLA1623B being a knot in the radio jet from VLA1623A appears strong when one looks at the 3.6-cm radio data (Bontemps & André 1997). There are several radio sources in a line apparently emanating from VLA1623A. At radio wavelengths VLA1623B is also much brighter than VLA1623A. This would tend to lend support to the hypothesis that the emission is arising from shocks in the jet.

Furthermore, close examination of Figure 1 shows that, whilst the position of VLA1623A appears constant with

wavelength, that of VLA1623B does not. The peak of the 7-mm data is offset from that of the 3.6-cm data, and both are offset from that of the 2.7-mm data. This would lend support to the hypothesis that this is not a single-peaked protostellar source.

However, the putative radio jet is not exactly coincident with the CO outflow (André et al. 1990; Dent et al. 1995), but rather is at an angle to it. Nevertheless, this may not be a problem. It could be that the 3.6-cm radio sources (including VLA1623B) could be the positions where a radio jet is interacting with the wall of the cavity caused by the CO outflow. In this hypothesis the heated dust emission seen at 2.7 mm would be shock-heated dust on the cavity wall.

Similar sources have been seen elsewhere by Maury et al. (2010). They see two apparent components to the protostar NGC1333-IRAS2A. They see something similar in L1448C. In this case the two components lie along a similar direction to the axis of the outflow (see their figure 3), but offset by a small angle, exactly as we see in VLA1623. They interpret the secondary source as a shock-heated portion of the outflow cavity wall.

5 CONCLUSIONS

We have presented mm and cm interferometer data of the Class 0 protostar VLA1623. We have detected the two components A & B that were previously known. The projected separation of the two components is ~ 170 AU. VLA1623A is a protostar with a circumstellar disc, whose radius lies in the range of $\sim 10\text{--}50$ AU. We estimate a limit to the disc mass of $\leq 0.13 M_{\odot}$. Excess emission at cm wavelengths is most likely due to optically thick free-free emission, but it could be indicating the onset of grain growth or planetesimal formation in the disc. The nature of VLA1623B remains a matter for debate. It lies along the line of the radio jet, and may be a shocked knot in the radio jet. Alternatively, it may be a binary component of the protostar. Further data are required to resolve this question.

ACKNOWLEDGEMENTS

MERLIN is a UK national facility operated by the University of Manchester at Jodrell Bank Observatory (JBO) on behalf of the UK Science and Technology Facilities Council (STFC). This work has benefited from research funding from the European Community's sixth Framework Programme under RadioNet R113CT 2003 5058187. The authors would like to thank the staff of the JBO for assistance during the taking and reducing of the MERLIN data. In particular, we thank Anita Richards and Tom Muxlow for their time and patience during the rather tricky data reduction phase. The VLA is operated by the American National Radio Astronomy Observatory (NRAO). NRAO is a facility of the American National Science Foundation (NSF), operated under co-operative agreement by Associated Universities, Inc. JMK acknowledges STFC for post-doctoral support through the Cardiff Astronomy Rolling Grant. The authors wish to thank the anonymous referee for helpful comments on an earlier draft of this paper.

REFERENCES

- Albrecht S., Reffert S., Snellen A. G., Winn J. N., 2009, *Nature*, 461, 373
- André P., 1994, in: Montmerle T., Lada C. J., Mirabel I. F., Tran Thanh Van J., eds, ‘The cold universe’, proceedings of ‘The XXVIIIth Rencontre de Moriond’, 179, Editions Frontières, Gif-sur-Yvette, France
- André P., Martin-Pintado J., Despois D., Montmerle T., 1990, *A&A*, 236, 180
- André P., Montmerle T., 1994, *ApJ*, 420, 837
- André P., Montmerle T., Feigelson E. D., Stine P. C., Klein K., 1988, *ApJ*, 335, 940
- André P., Ward-Thompson D., Barsony M., 1993, *ApJ*, 406, 122 – AWB93
- André P., Ward-Thompson D., Barsony M., 2000, in: Mannings V., Boss A. P., Russell S. S., eds, ‘Protostars and Planets IV’, 59, University of Arizona Press, Tucson, Arizona, USA – AWB00
- Bontemps S., André P., 1997, in: Malbet F., Castets A., eds, ‘Low mass star formation – from infall to outflow’, poster proceedings of IAU Symposium, 182, 63, Observatoire de Grenoble, France
- Bontemps S., Ward-Thompson D., André P., 1996, *A&A*, 314, 477
- Brauer F., Dullemond C. P., Henning T., 2008, *A&A*, 480, 859
- Bridle A. H., Greisen E. W., 1994, ‘The NRAO AIPS project – a summary’, National Radio Astronomy Observatory, Charlottesville, Virginia, USA
- Carrasco-Gonzalez C., Rodriguez L. F., Anglada G., Curiel S., 2009, *ApJ*, 693, L86
- Curiel S., Ho P. T. P., Patel N. A., Torrelles J. M., Rodriguez L. F., Trinidad M. A., Canto J., Hernandez L., Gomez J. F., Garay G., Anglada G., 2006, *ApJ*, 638, 878
- Dent W. R. F., Matthews H. E., Walther D. M., 1995, *MNRAS*, 277, 193
- Dutrey A., Guilloteau S., Pietu V., Chapillon E., Gueth F., Henning T., Launhardt R., Pavlyuchenkov Y., Schreyer K., Semenov D. 2008, *A&A*, 490, L15
- Girart J. M., Rao R., Marrone D. P., 2006, *Science*, 313, 812
- Greaves J. S., Richards A. M. S., Rice W. K. M., Muxlow T. W. B., 2008, *MNRAS*, 391, L74
- Guilloteau S., Dutrey A., Pety J., Gueth F., 2008, *A&A*, 478, L31
- Holland W. S., Greaves J. S., Ward-Thompson D., André P., 1996, *A&A*, 309, 267
- Henriksen R., André P., Bontemps S., 1997, *A&A*, 323, 549
- Kirk J. M., Ward-Thompson D., André P., 2005, *MNRAS*, 360, 1506
- Lada C. J., 1987, in: Peimbert M., Jugaku J., eds, ‘Star-forming regions’, IAU Symposium 115, 1, Reidel, Dordrecht
- Leous J. A., Feigelson E. D., André P., Montmerle T., 1991, *ApJ*, 379, 683
- Looney L. W., Mundy L. G., Welch W. J., 2000, *ApJ*, 529, 477
- Looney L. W., Mundy L. G., Welch W. J., 2003, *ApJ*, 592, 255
- Mamajek E. E., 2008, *Astron. Nachr.*, 329, 10
- Maury A. J., André P., Hennebelle P., Motte F., Stamatellos D., Bate M., Belloche A., Duchene G., Whitworth A., 2010, *A&A*, 512, A40
- Pudritz R. E., Wilson C. D., Carlstrom J. E., Lay O. P., Hills R. E., Ward-Thompson D., 1996, *ApJ*, 470, L123
- Reynolds S. P., 1986, *ApJ*, 304, 713
- Schaefer G. H., Dutrey A., Guilloteau S., Simon M., White R. J., 2009, *ApJ*, 701, 698
- Simpson R. J., Nutter D. J., Ward-Thompson D., 2008, *MNRAS*, 391, 205
- Stamatellos D., Maury A., Whitworth A., Andre P., 2011, *MNRAS*, in press, arXiv1012.3455
- Torrelles J. M., Patel N. A., Curiel S., Estalella R., Gomez J. F., Rodriguez L. F., Canto J., Anglada G., Vlemmings W., Garay G., Raga A. C., Ho P. T. P., 2011, *MNRAS*, 410, 627
- Ward-Thompson D., 2007, in: Griffin M. J., Hargrave P. C., Parker T. J., Wood K. P., eds, ‘Joint 32nd International Conference on Infrared and Millimeter Waves and 15th International Conference on Terahertz Electronics’, 720, IEEE, Piscataway, New Jersey, USA
- Ward-Thompson D., André P., Lay O. P., 2004, in: Penny A., Artymowicz P., Lagrange A. M., Russell S., eds, ‘Planetary Systems in the Universe: Observation, Formation and Evolution’, IAU Symposium, 202, 393, Astronomical Society of the Pacific Conference Series, San Francisco, USA
- Welch W. J., Webster Z., Mundy L., Volgenau N., Looney L., 2004, in: Norris R. P., Stootman F. H., eds, ‘Bioastronomy 2002 – life among the stars’, IAU Symposium, 213, 59, Astronomical Society of the Pacific Conference Series, San Francisco, USA
- Wilking B. A., Lada C. J., Young E. T., 1989, *ApJ*, 340, 823
- Wright A. E., Barlow M. J., 1975, *MNRAS*, 170, 41
- Qi C., Ho P. T. P., Wilner D. J., Takakuwa S., Hirano N., Ohashi N., Bourke T. L., Zhang Q., Blake G. A., Hogerheijde M., Saito M., Choi M., Yang J., 2004, *ApJ*, 616, L11